EPR of Pernigraniline Base: The Structure of Neutral Solitons

S.M. Long
Department of Physics, The Ohio State University, Columbus, Ohio 43210-1106

Y. Sun* and A.G. MacDiarmid
Department of Chemistry, University of Pennsylvania, Philadelphia, Pennsylvania 19104

A.J. Epstein
Department of Physics and Department of Chemistry, The Ohio State University, Columbus, Ohio 43210-1106
(Received 11 March 1994)

EPR hyperfine spectra of pernigraniline base (PNB) powder and solutions provide a direct measure of the internal structure of neutral soliton defects, S^0. The π-electron spin density resides largely on a central nitrogen, $|\rho_N| \approx 0.36$, and adjacent phenyl rings where $|\rho_C| \approx 0.125$ and $|\rho_C| \lesssim 0.04$ for carbons meta and ortho to the nitrogen center, respectively. Calculations based on a Hubbard model yield an estimate of the on-site Coulomb repulsion $U \sim 2.5$ eV similar to that of S^0 in *trans*-polyacetylene. The smaller diffusion coefficient for S^0 in PNB ($D_\parallel < 10^{-6}$ cm^2 sec^{-1}) is contrasted to that of solitons in *trans*-polyacetylene ($D_\parallel \sim 10^{-4}$ cm^2 sec^{-1}).

PACS numbers: 76.30.−v, 71.20.Hk, 71.50.+t, 73.20.Dx

Despite the importance of experimentally establishing the internal spin distribution of defects in conjugated polymers for comparison to theoretical predictions, few studies are reported. Electron nuclear double resonance (ENDOR) has been successful at providing insight into the internal spin density distribution of neutral solitons (S^0) in *trans*-$(CH)_x$ [1] and polarons in poly(paraphenylene vinylene) [2]. We report in this Letter the first use of electron paramagnetic resonance (EPR) hyperfine structure in solution to determine the internal spin density distribution of defects in a conjugated polymer, neutral solitons S^0 in pernigraniline base (PNB). The S^0 defects in PNB are determined to be of a benzenoid-nitrogen-benzenoid configuration, and not the (higher energy) quinoid-nitrogen-quinoid configuration. Model fits to the hyperfine spectrum provide good agreement with the predicted spin distribution of S^0 of Su and Epstein [3]. An improvement is obtained if an on-site Coulomb repulsion (Hubbard U) of ~ 2.5 eV is included in the calculation of S^0 spin distribution. The Coulomb repulsion in PNB is determined to be similar to that of *trans*-$(CH)_x$ [1]. An upper limit for the S^0 diffusion rate is obtained and contrasted with the more rapid diffusion of polarons and solitons in emeraldine base in solution and in *trans*-$(CH)_x$, respectively.

Pernigraniline base polymer (inset, Fig. 1) is the second polymer, in addition to *trans*-$(CH)_x$, in which soliton defects may exist [3–6]. PNB undergoes bond-length and ring-torsion dimerization with alternation between benzenoid and quinoid rings resulting in a twofold degenerate ground state [4,6]. dos Santos and Brédas proposed that PNB can support two types of charged solitonic distortions, both centered on nitrogen atoms, one having an aromatic ring geometry and the other a quinoid ring structure [4]; these have been experimentally observed via millisecond photoinduced absorption spectroscopy [7]. Theoretical studies by Su and Epstein [3] and Baranowski *et al.* [8] have focused on the stability and dynamics of the Peierls state in pernigraniline base. Using the tight-binding model, Su and Epstein found the structure of neutral solitons ($S = 1/2$) to be of the BNB (B ≡ benzenoid, N ≡ nitrogen) form with the wave function centered symmetrically on a nitrogen site and primarily localized to the two adjacent rings [3]. This is in contrast to solitons in *trans*-$(CH)_x$ where the wave function extends over approximately 14 repeat units [9]. Recently neutral solitons were detected in PNB via photoinduced absorption and light induced EPR measurements [10].

EPR can directly probe hyperfine interactions associated with the spin distribution of defects; though dipolar broadening in the solid state tends to wash out any resolvable fine structure. In contrast, for solutions dipolar broadening interactions are effectively averaged to zero by rapid tumbling motion when $\tau_c^{-1} \gg \omega_p$ where τ_c^{-1} is the molecular tumbling rate and ω_p is the mag-

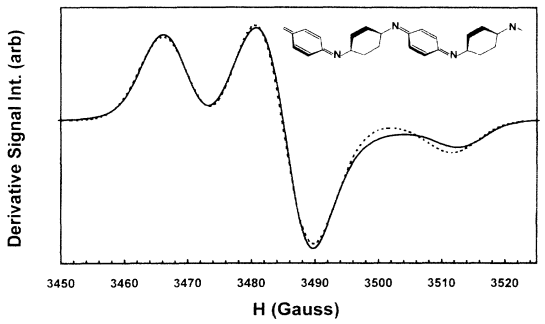

FIG. 1. Experimental EPR spectrum of PNB powder (solid line) at room temperature with modulation amplitude 0.477 G and microwave power of 2.0 mW (unsaturated regime). Simulated powder spectrum based on a single anisotropic N^{14} hyperfine interaction (dashed line). Inset: Idealized chemical structure of pernigraniline base (PNB) polymer.

0031-9007/94/72(20)/3210(4)$06.00

nitude of the broadening interaction. The linewidth is then $\Delta\omega \sim \omega_p^2\tau_c$ and hyperfine interactions greater than $\Delta\omega$ can be resolved. Rapid motional narrowing also effectively averages anisotropies in the hyperfine splitting tensor $\overleftrightarrow{A}$ and g tensor $\overleftrightarrow{g}$ greatly simplifying the spectra which then depend only on the isotropic values given by $A_{\rm iso} = (1/3)\mathrm{Tr}\langle\overleftrightarrow{A}\rangle$ and $g_{\rm iso} = (1/3)\mathrm{Tr}\langle\overleftrightarrow{g}\rangle$, respectively. The insolubility of $(CH)_x$ and most other electronic polymers has made it impossible to study S^0 and charged polarons using this technique. The improvement in the synthesis and solubility of PNB have provided a unique opportunity to utilize solution EPR to probe S^0 defects.

PNB powder samples were synthesized via the oxidation of emeraldine base with an acetic acid solution of *m*-chloroperbenzoic acid followed by deprotonation with triethlyamine [10]. For the present study N-methly-2-pyrrolidinone (NMP) and dioxane solvents were chosen. The PNB powder was finely ground and solvent added. Only a small percentage of the PNB powder sample was found to be soluble and a 0.45 μm Teflon filter was necessary to remove the remaining undissolved particulates. The low percentage of soluble PNB powder may be a result of a distribution in the molecular weight and/or crystallinity of the PNB sample similar to emeraldine base [11]. The EPR solid state spectra of insoluble PNB and dried solutions of PNB were nearly identical. Thus comparison of the PNB defect observed in solution and the "as made" PNB powder (containing soluble and insoluble PNB) spectra is justified.

The room temperature cw-EPR spectra were obtained with a Bruker ESP300 *X*-band spectrometer using a standard TE_{102} microwave cavity. For NMP, a high-loss ($\epsilon = 32$) solvent, a flat quartz cell with an inner thickness of 0.5 mm and width 4.75 mm was used to position the sample in the cavity along the planar node of the electric field to minimize dielectric loss. For dioxane, a low-loss ($\epsilon = 2.29$) solvent, a 4 mm i.d. quartz EPR tube was used. Because of dioxane's low dielectric loss and the larger effective sample volume obtainable the highest resolution spectra were obtained with this solvent.

The room temperature EPR spectrum of PNB powder, Fig. 1, has three partially resolved peaks spanning ~ 60 G characteristic of a single interaction with a spin one nuclei with anisotropic $\overleftrightarrow{g}$ and $\overleftrightarrow{A}$ tensors. The similarity to the photoinduced EPR line shape [10] demonstrates these are "intrinsic" soliton defects. The simulated powder pattern (Fig. 1), determined using a modified version of QCPE Program No. 265 [12], corresponds to an electronic spin 1/2 interacting with a single spin one nuclei where $A_x = 2.3$ G, $A_y = 2.3$ G, $A_z = 22.4$ G, $g_x = 2.0076$, $g_y = 2.0061$, and $g_z = 2.0029$. The simulation required a Gaussian instead of a Lorentzian broadening function with a peak-to-peak linewidth of 8.2 G to achieve a good fit, an indication of additional hyperfine interactions which would be evident in solution spectra. The only spin one nuclei in PNB are nitrogen.

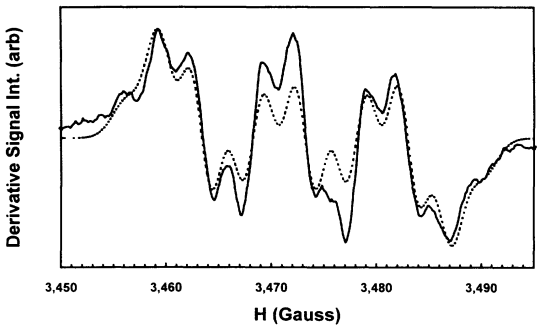

FIG. 2. EPR spectrum of PNB in dioxane (solid line). Simulated spectra based on hyperfine interaction with one N^{14} and four H^1 nuclei (dashed line).

Thus from the powder pattern the isotropic hyperfine splitting constant is $|A_{\rm N}| = (2.3 + 2.3 + 22.4)/3 = 9.0$ G. The g values in the powder pattern were calibrated against a DPPH standard; the isotropic g value is $g_{\rm iso} = (2.0076 + 2.0061 + 2.0029)/3 = 2.0055$.

The EPR solution spectrum of PNB in dioxane is shown in Fig. 2. To achieve an acceptable signal to noise ratio a microwave power of 5 mW was required, but resulted in no appreciable saturation of the resonance. The spectra of PNB in NMP was found to be identical to that of PNB in dioxane, thus no solvent effects were detected. Measurement of the g value against DPPH gave $g_{\rm iso} = 2.0057$, in agreement with the PNB powder result. The experimental spectrum is readily modeled in the rapid motional narrowing limit in terms of hyperfine splitting due to a single N^{14} ($I = 1$) and four equivalent H^1 ($I = 1/2$) hyperfine interactions, Fig. 2. The absolute values of the isotropic hyperfine splitting constants are found to be $A_{\rm N} = 9.8$ G and $A_{\rm H} = 3.0$ G. A Gaussian broadening function instead of the usual Lorentzian function was also necessary and indicates the presence of unresolved hyperfine structure. Based on the chemical structure of PNB it is assumed this results from interactions with the four remaining hydrogens on the adjacent rings and possibly the two adjacent nitrogens. Assuming the Gaussian broadening function ($\Delta H_{pp} = 3.0$ G) is associated with four roughly equivalent hydrogens (line intensity pattern 1:4:6:4:1) a splitting constant of ~ 1 G is indicated. If the broadening is due instead to two roughly equivalent nitrogens (line intensity pattern 1:2:3:2:1) a splitting constant of ~ 1 G is also indicated. Thus $|A_X| \lesssim 1$ G is an upper limit on all unresolved hyperfine interactions.

McConnell described [13] a linear relationship between the hyperfine splitting and the unpaired p_z-electron densities for π-type organic radicals, $A_i = Q_i\rho_i$, where ρ_i is the π-electron spin density, Q_i an empirically found spin polarization constant, and A_i the measured hyperfine splitting constant for the ith atomic site. $Q_{\rm N}$ for nitrogen sites range from 23 to 30 G depending on the local configuration. Taking the nitrogen in PNB as hav-

ing sp^2 hybridized orbitals and noting that no additional splitting is observed to indicate additional atoms bonded to the nitrogen [14], we deduce that the nitrogen site is unprotonated possessing a lone pair in a σ orbital. For nitrogen with this configuration a typical value of $Q_N = 27.3$ G has been suggested [15]. The corresponding $\mid \rho_N \mid$ is estimated as $9.8/27.3 = 0.36$ $(+0.07, -0.03)$. Assuming the hydrogen hyperfine splitting, $\mid A_H \mid = 3.0$ G, is due to protonated carbon sites on the adjacent phenyl rings the π-electron spin densities can similarly be determined. (Note: no C^{13} hyperfine splitting was observable in our spectra.) Based on the effects of excess charge on Q values [16] we use $Q_{CH} = -24.1$ G, the average of the anion -22.5 G [17] and cation -25.7 G [18] polarization constants for neutral phenyl rings. The corresponding π-electron spin densities for four of the eight phenyl ring carbon sites are $\mid \rho_C \mid = 3.0/24.1 = 0.125 \pm 0.01$. For the unresolved hyperfine splitting, $\mid A_X \mid \lesssim 1$ G, we assume a representative spin polarization constant of $Q_X = 25$ G. The limit on the corresponding π-electron spin densities, whether due to additional nitrogen or protonated carbon sites on the rings, is $\mid \rho_X \mid \lesssim 1/25 = 0.04$. From the symmetry of PNB (assuming a linear geometry of the ring-N-ring) the four carbons (site 2) meta to the central nitrogen (site 0) are equivalent and similarly the four carbons (site 3) ortho are equivalent. Assuming the higher π-electron spin densities occur at the sites closest to the central nitrogen we assign the four carbons at site 2 each a density of $\mid \rho_C \mid = 0.125$ and the four carbons at site 3 each $\mid \rho_X \mid \lesssim 0.04$, Fig. 3(b).

dos Santos and Brédas proposed [4] that PNB could support two types of soliton distortions, one a BNB geometry, the other a quinoid-nitrogen-quinoid (QNQ) geometry, with an antinode and node for their wave functions at the central nitrogen, respectively. For an isolated neutral soliton the BNB geometry is energetically most stable. The strong nitrogen hyperfine splitting in our spectra clearly reflects the BNB-S^0 geometry. We see no direct evidence for the presence of the QNQ type soliton. However, the differences between our experimental and simulated solution spectra indicate the possibility of an additional weaker signal underlining the center region of the spectra.

Based on a tight-binding Hamiltonian, Su and Epstein [3] calculated the gap state wave function for a BNB type neutral soliton as primarily localized to a central nitrogen and immediate adjacent rings. The probability of finding an unpaired electron at the single central nitrogen was found to be 0.45 in fair agreement with our experimentally determined value of $\mid \rho_N \mid = 0.36$. The spectral width of a motionally narrowed resonance is a measure of unpaired π-electron distribution, $\Delta H_{sw} = 2\sum_{\langle i \rangle} I_i \mid Q_i \mid\mid \rho_i \mid$ where $\langle i \rangle$ is the sum over all nitrogen and carbon-hydrogen hyperfine sites and I_i is the nuclear spin quantum number. Using the S^0 gap state wave function, $\rho_i = \mid \Phi_i \mid^2$, reported by Su and Epstein we calculate $\Delta H_{sw} = 31.3$ G, significantly smaller than

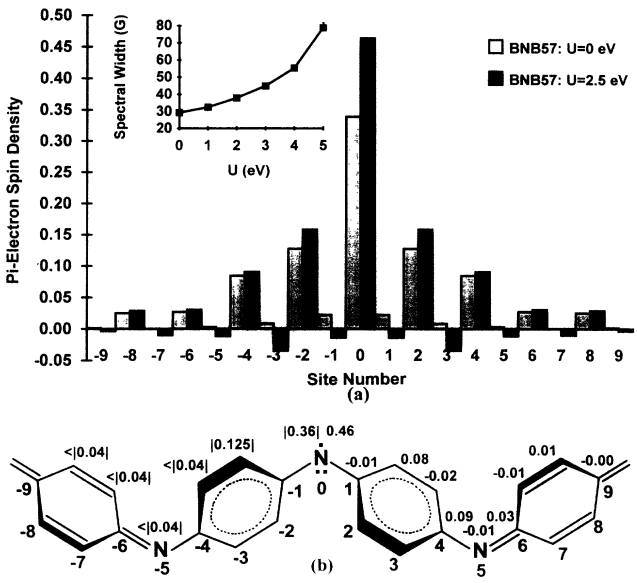

FIG. 3. (a) Calculated π-electron spin density distribution showing effects of Coulomb repulsion. Inset: plot of spectral width as a function of U. (b) π-electron spin density distribution determined from experimental hyperfine splitting constants (numbers to left) and theoretically determined values for $U = 2.5$ eV (numbers to right).

$\Delta H_{sw} \sim 41$ G for the experimental solution spectrum. As $\Delta H_{sw} \propto \sum_i \mid \rho_i \mid$ where the sum is over all hyperfine sites this difference in the spectral width can be accounted for by Coulomb repulsion resulting in negative spin densities at some sites and compensating positive spin densities at other sites.

A sum of all π-electron spin densities should equal 1 corresponding to a total spin of 1/2. Summing the experimental spin densities assuming only positive values gives $\mid 0.36 \mid +4 \mid 0.125 \mid +4 \mid 0.04 \mid \approx 1.02$. This sum is only a partial sum of the total spin density despite its coincidental value of $\sim$1. This sum does not include the four carbons at sites 1 and 4 where a sizable spin density is expected as well as sites beyond the first adjacent rings. It is unreasonable to expect these sites to have a zero or even small fraction of the total spin density. (Based on Su's and our models it is expected that $\sim$30% of the total spin density lies on sites with no hyperfine interaction.) Thus sites with negative spin densities must be present in the BNB-S^0 density distribution in order for the total spin density to sum to one.

We calculate the π-electron spin density for a BNB-S^0 within the Hubbard model. The corresponding Hamiltonian is

$$H = \sum_{n,\sigma} V_n c^\dagger_{n,\sigma} c_{n,\sigma} + \sum_{i,j,\sigma} t_{i,j} (c^\dagger_{i,\sigma} c_{j,\sigma} + \text{c.c.}) + \sum_i U_i n_{i,\uparrow} n_{i,\downarrow}$$

where the last term is the "on-site" Coulomb repulsion (Hubbard "U"). Using the bond orders, $t_{i,j}$, and site energies V_n utilized by Su and Epstein for the BNB-S^0 (no Coulomb repulsion) we calculated the self-consistent π-

electron spin density for values of U up to 9 eV (assuming $U_N = U_C$), and ΔH_{sw} as a function of U, inset Fig. 3(a). The best fit to the experimental spectral width, ~ 41 G, corresponds to $U = 2.5$ eV. In Fig. 3(a) our calculated π-electron spin density for $U = 0$ and 2.5 eV is shown. The result of Coulomb repulsion is to increase the densities on even numbered sites and compensate with negative densities on odd sites. This is precisely the same behavior calculated for S^0 with $U = 3$ eV in linear *trans*-$(CH)_x$, and observed by ENDOR [1]. Though $U_{(CH)_x}$ and U_{PNB} are approximately equal, the small bandwidth for PNB implies the greater importance for the latter system. The calculated densities on the central nitrogen and meta carbons are somewhat larger and smaller, respectively, than observed. A decrease in the torsion angle of the adjacent rings of $\sim 15°$ from that of the assumed Su and Epstein geometry (from a torsion angle of 44° to $\sim 30°$) would result in a decrease in spin density ($\sim 25\%$) on the central nitrogen and an increase in that of the rings while decreasing ΔH_{sw} by only $\sim 5\%$.

In *trans*-$(CH)_x$ solitonic defects are highly mobile having an intrachain hopping rate of $\tau_c^{-1} \sim 10^{11}$ sec^{-1} (diffusion coefficient $D_{\|} \sim 10^{-4}$ cm^{2}sec^{-1}) at room temperature [19]. This mobility gives rise to motional narrowing or averaging of the hyperfine interactions and results in a very narrow linewidth, $\Delta H_{1/2} < 1$ G. In PNB there is no evidence of any motional narrowing of the hyperfine interactions in either the powder or solution spectra. Thus the solitonic defects (experimentally 1 per 100 to 1 per 3000 rings dependent on the preparation) must be immobile or slow moving. Based on the narrowing condition and the linewidth, $\Delta H \approx 20$ G, the intrachain hopping rate must be $\tau_c^{-1} < (\hbar/g\beta\Delta H)^{-1} \sim 10^8$ sec^{-1} (diffusion coefficient $D_{\|} < 10^{-6}$ cm^2 sec^{-1}). We attribute lower mobility of S^0 in PNB to the short localization length of S^0 and the role of ring torsion angle changes. A soliton must skip one nitrogen during a move from one site to the next; the geometry requires the interchange of a benzenoid and quinoid (i.e., BQB·BQBQ to BQBQB·BQ) with concomitant ring-angle and bond length changes. This required structural reordering introduces a substantial barrier to motion. In contrast for polyacetylene the solitonic distortion is spread out over 14 carbon atoms, i.e., much larger than the distance that it moves in a hop, 2 carbons, and its motion involves only translation of C atoms. The more delocalized solitonic distortion results in a lower energy barrier to motion. This view is supported by the absence of fine structure in the EPR of polarons in nondegenerate emeraldine base (EB) in solution (solution linewidth $\simeq 1.7$ G, $\tau_c^{-1} \sim 10^{11}$ sec^{-1}, and $D_{\|} \sim 10^{-3}$ cm^2 sec^{-1}) where polaron motion involves smaller ring torsion angle changes.

In conclusion the solubility of PNB enabled the direct measurement via EPR of the internal spin structure of S^0 defects in the degenerate ground state polymer PNB. Analysis supports a BNB S^0 structure similar to that proposed theoretically with the addition of a significant U of ~ 2.5 eV. The slow diffusion of these S^0 defects is attributed to the role of ring motion and contrasted with more rapid diffusion of polarons in nondegenerate EB and solitons in *trans*-$(CH)x$.

We thank K.R. Cromack, K.A. Coplin, S. Jasty, and M.M. Steiner for helpful discussions. This work was funded in part by the Office of Naval Research.

* Present address: Rohm and Haas Company, Springhouse, PA 19477.

[1] H. Thomann, L.R. Dalton, Y. Tomkiewicz, N.S. Shiren, and T.C. Clarke, Phys. Rev. Lett. **50**, 533 (1983).
[2] S. Kuroda, T. Noguchi, and T. Ohnishi, Phys. Rev. Lett. **72**, 286 (1994).
[3] W.P. Su and A.J. Epstein, Phys. Rev. Lett. **70**, 1497 (1993).
[4] M.C. dos Santos and J.L. Brédas, Phys. Rev. Lett. **62**, 2499 (1989).
[5] J.L. Brédas, C. Quattrocchi, J. Libert, A.G. MacDiarmid, J.M. Ginder, and A.J. Epstein, Phys. Rev. B **44**, 6002 (1992).
[6] J.M. Ginder and A.J. Epstein, Phys. Rev. Lett. **64**, 1184 (1990); Phys. Rev. B **41**, 10674 (1990).
[7] J.M. Leng, J.M. Ginder, R.P. McCall, H.J. Ye, Y Sun, S.K. Manohar, A.G. MacDiarmid, and A.J. Epstein, Phys. Rev. Lett. **68**, 1184 (1992).
[8] D. Baranowski, H. Buttner, and J. Voit, Phys. Rev. B **45**, 10990 (1992).
[9] W.P. Su, J.R. Schrieffer, and A.J. Heeger, Phys Rev. Lett. **42**, 1698 (1979).
[10] K.A. Coplin, S. Jasty, S.M. Long, S.K. Manohar, Y. Sun, A.G. MacDiarmid, and A.J. Epstein, preceding Letter, Phys. Rev. Lett. **72**, •••• (1994).
[11] M.E. Jozefowicz, A.J. Epstein, J.P. Pouget, J.G. Masters, A. Ray, Y. Sun, X. Tang, and A.G. MacDiarmid, Synth. Met. **41-43**, 723 (1991).
[12] Powder Spectrum EPR Simulation: Quantum Chemistry Program Exchange (QCPE) Program No. 265 incorporating a *Downhill Simplex* algorithm for parameter optimization and modified by D.R. Duling.
[13] H.M. McConnell, J. Chem. Phys. **24**, 764 (1956).
[14] Atoms with spin zero nuclei such as oxygen could be bound to the nitrogen (as in nitroxide radicals) without significantly changing the character of the spectrum.
[15] C.L. Talcott and R.J. Myers, Mol. Phys. **12**, 549 (1967).
[16] J.P. Colpa and J.R. Bolton, Mol. Phys. **6**, 273 (1963).
[17] J.R. Bolton, Mol. Phys. **6**, 219 (1963).
[18] M.K. Carter and G. Vincow, J. Chem. Phys. **47**, 292 (1967).
[19] B.R. Weinberger, E. Ehrenfreund, A. Pron, A.J. Heeger, and A.G. MacDiarmid, J. Chem. Phys. **72**, 4749 (1980).

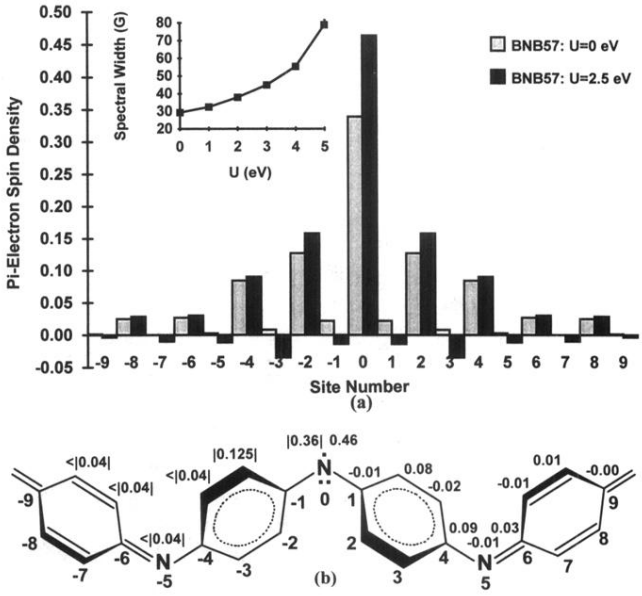

FIG. 3. (a) Calculated π-electron spin density distribution showing effects of Coulomb repulsion. Inset: plot of spectral width as a function of U. (b) π-electron spin density distribution determined from experimental hyperfine splitting constants (numbers to left) and theoretically determined values for $U = 2.5$ eV (numbers to right).